The Influence of Divalent Cations on the Dynamic Properties of Actin Filaments: A Spectroscopic Study

G. Hild,* M. Nyitrai,† J. Belágyi,‡ and B. Somogyi*†

*Department of Biophysics, †Research Group of the Hungarian Academy of Sciences at the Department of Biophysics, and ‡Central Research Laboratory, University Medical School of Pécs, P.O.B. 99. H-7601 Pécs, Hungary

ABSTRACT The principal aim of this investigation was to study the change of the protein flexibility and/or conformational properties of actin filaments upon the replacement of Ca^{2+} by Mg^{2+}. The temperature dependence of the fluorescence lifetime and the anisotropy decay of *N*-(iodoacetyl)-*N′*-(5-sulfo-1-naphthyl)ethylenediamine (IAEDANS) attached covalently to the Cys^{374} residue of actin were measured. Saturation transfer electron paramagnetic resonance (ST-EPR) experiments were also carried out using *N*-(1-oxyl-2,2,6,6-tetramethyl-4-piperidinyl)-maleimide (MSL) attached to the same residue (Cys^{374}). The Arrhenius analysis of the temperature dependence of the fluorescence lifetimes shows that for Mg-F-actin, both the activation energy (E^*) and the frequency factor (A) are smaller than they are for Ca-F-actin. The longer rotational correlation times resolved in the fluorescence experiments are larger in the Mg^{2+}-loaded form of the actin filament between 6°C and 28°C, but this difference becomes negligible above 28°C. The results of saturation transfer electron paramagnetic resonance measurements on maleimide spin-labeled actin filaments indicate that the replacement of Ca^{2+} by Mg^{2+} induced a decrease of the mobility of the label on the sub-millisecond time scale. Based upon these results, we concluded that the filaments polymerized from Ca-actin are more flexible than the filaments of Mg-actin.

INTRODUCTION

The conformational state and flexibility of the actin filament play an important role in muscle contraction (Prochniewicz and Yanagida, 1990; Rayment et al., 1993). The rotational correlation times characteristic of different modes of internal motion within the actin filament are generally distributed across a wide time scale from the nanosecond to the millisecond range. Depending on the experimental method applied, various types of these intramolecular motions can be identified.

The relaxation time of the actin filament bending motion is on the order of 10 ms (Fujime and Ishiwata, 1971). The results of saturation transfer electron paramagnetic resonance (ST-EPR) experiments revealed that a spin label rigidly attached to F-actin has a correlation time in the range of 10^{-4} s (Thomas et al., 1979; Hegyi et al., 1988). The correlation time expected for the uniaxial rotation of the F-actin molecule as a whole is $\sim 20-40$ μs (Kawamura and Maruyama, 1970; Tawada et al., 1978), which range is therefore comparable with the range obtained from the data of saturation transfer EPR experiments. Mihashi and coworkers concluded from transient absorption anisotropy experiments that the actin filaments are more flexible in twisting motion than in bending motion (Mihashi et al., 1983). The correlation times resolved in these measurements was in the microsecond range, reflecting some kind of internal motion of F-actin. The torsional motion is faster than the above modes and has been studied by fluorescence techniques (Mihashi and Wahl, 1975; Wahl et al., 1975; Kawasaki et al., 1976; Tawada et al., 1978; Ikkai et al., 1979; Miki et al., 1982a,b). The longer correlation times were resolved in the range of several hundreds of nanoseconds according to fluorescence anisotropy decay measurements.

The binding of Ca^{2+} to the actin in the presence of 100 mM KCl increased the mobility of the fluorescence label attached to the Cys^{374} residue of the protein (Miki et al., 1982a,b). The authors concluded that the change to the longer correlation time must be due to a conformational transition. Recent results of nuclear magnetic resonance (NMR) experiments on actin filaments revealed cation-dependent changes in the mobility of the *N*-terminal segment (first 21 amino acids) of actin (Heintz et al., 1996). The torsional rigidity of actin filaments, however, is larger when Ca^{2+} occupies the high affinity binding site than when Mg^{2+} occupies the site (Yasuda et al., 1996). Orlova and Egelman found that the bending flexibility of filaments polymerized from Mg-actin is greater than that of filaments polymerized from Ca-actin (1993). A "bridge of density" was found between the two strands of filament when the high affinity cation-binding sites were occupied by Ca^{2+}, whereas this "bridge of density" was not detected in Mg-F-actin (Orlova and Egelman, 1995). However, other laboratories found essentially no cation dependence of the flexibility of filaments using either dynamic light scattering measurements (Scharf and Newman, 1995), or other techniques (Isambert et al., 1995; Steinmetz et al., 1997) to determine the persistence length of filaments. Direct measurement of the flexibility of single actin filaments corroborates this conclusion (Yasuda et al., 1996). The apparent inconsistency of these data was attributed in part to subtle differences in the polymerization conditions (i.e., in terms of nucleotide and cation compositions and/or concentrations) (Steinmetz et al., 1997).

Received for publication 14 April 1998 and in final form 3 September 1998.

Address reprint requests to Dr. Bela Somogyi, H-7624 Pécs, Szigeti str. 12, Pécs, Hungary. Tel./Fax: 36–72-314–017; E-mail: sombel@apacs.pote.hu

0006-3495/98/12/3015/08 $2.00

Accordingly, there is no consistent picture of the effect of bound metal ion (i.e., Ca^{2+}, Mg^{2+}) on the flexibility of actin filaments. In this paper we direct attention to the effect of replacement of Mg^{2+} with Ca^{2+} on the flexibility and/or conformational properties of the actin filament, using fluorescence and EPR spectroscopic methods. We measured the temperature dependence of the fluorescence lifetime and the anisotropy decay of *N*-(iodoacetyl)-*N′*-(5-sulfo-1-naphthyl) ethylenediamine (IAEDANS) and the saturation-transfer EPR data obtained by using MSL, both attached covalently to the Cys^{374} at the C-terminus on subdomain-1 of actin. These spectroscopic experiments provided evidence that filaments polymerized from Mg-actin are more rigid than filaments of Ca-actin.

MATERIALS AND METHODS

Materials

KCl, $MgCl_2$, $CaCl_2$, Tris, glycogen, IAEDANS, MSL, and EGTA were obtained from Sigma Chemical Co. (St. Louis, MO). ATP and α-mercaptoethanol were obtained from Merck (Darmstadt, Germany), and NaN_3 from Fluka (Buchs, Switzerland).

Protein preparation

Acetone-dried powder of rabbit skeletal muscle was obtained as described earlier (Feuer et al., 1948). Rabbit skeletal muscle actin was prepared according to Spudich and Watt (1971) and stored in a buffer containing 2 mM Tris-HCl (pH 8.0), 0.1 mM ATP, 0.1 mM $CaCl_2$, and 0.02% NaN_3 (buffer A). The concentration of G-actin was determined spectrophotometrically using the absorption coefficient of 0.63 mg ml^{-1} cm^{-1} at 290 nm (Houk and Ue, 1974), with a Shimadzu UV-2100 type spectrophotometer. Relative molecular mass of 42,300 was used for G-actin (Elzinga et al., 1973).

Fluorescence labeling of actin

Actin labeled fluorescently with IAEDANS at Cys^{374} was prepared according to the method of Miki and co-workers (1987). 2 mg/ml F-actin (in buffer A without α-mercaptoethanol, supplemented with 100 mM KCl and 2 mM MgCl2) was incubated with tenfold molar excess of IAEDANS at room temperature for 1 h. The label was first dissolved in dimethylformamide; its final concentration in the labeling solution did not exceed 0.6% (v/v). The solution was diluted $\sim 50\times$ with buffer A before being added to the protein. Labeling was terminated with 1 mM α-mercaptoethanol. After ultracentrifugation of the sample at 100,000 *g* the pellet was incubated in buffer A for 1 h and gently homogenized with a Teflon homogenizer. The homogenated sample was exhaustively dialyzed overnight against buffer A at 4°C. The concentration of fluorescent dye in the protein solution was determined by using the absorption coefficient of 6100 M^{-1} cm^{-1} at 336 nm for actin-bound IAEDANS (Hudson and Weber, 1973). The extent of labeling was determined to be 0.85 $\pm$ 0.05 mol/mol of actin monomer.

Spin labeling of actin

G-actin was polymerized by adding KCl and $MgCl_2$ to final concentrations of 100 and 2 mM, respectively. Actin was labeled in F-form with MSL as described earlier (Mossakowska et al., 1988). One mole of spin label per mole of actin monomer was reacted for 90 min over ice. Unreacted labels were removed as described above. The degree of labeling ranged from 0.2–0.55 mol/mol of actin.

Cation exchange on actin

Mg-G-actin was prepared from Ca-G-actin following the method of Strzelecka-Golaszewska and colleagues (1993). The protein solution was dialyzed overnight against buffer A (in which the concentration of $CaCl_2$ was 50 μM). EGTA and $MgCl_2$ were added from stock solutions to reach final concentrations of 0.2 mM and 0.1 mM, respectively, in the protein solution. The sample was incubated for 10 min at room temperature. Mg-F-actin and Ca-F-actin were prepared from Mg-G-actin and Ca-G-actin, respectively, by the addition of 100 mM KCl and 2 mM of the appropriate cation ($MgCl_2$ or $CaCl_2$) to the sample. Incubation time was 2 h for Mg-F-actin and at least 4 h for Ca-F-actin at room temperature.

For saturation-transfer EPR measurements the concentration of F-actin was at least 100 μM. In some cases the precipitation of the protein was observed when a highly concentrated solution of salts (2–3 M solution of KCl, $CaCl_2$, or $MgCl_2$) was added to the Mg-G-actin or Ca-G-actin to initialize polymerization. To avoid this condensation, we obtained the filaments with different cations by dialysing the samples in the appropriate polymerization buffer (i.e., buffer A supplemented with 100 mM KCl, 0.2 mM EGTA, and 2 mM $MgCl_2$ for Mg-F-actin, or buffer A with 100 mM KCl and 2 mM $CaCl_2$ for Ca-F-actin). Polymerization was carried out overnight at 4°C.

Light-scattering experiments

The polymerization capability of Ca-actin and Mg-actin was examined by measuring the change in the intensity of Rayleigh-scattered light on actin during the polymerization process. The experiments were performed on a Perkin-Elmer LS50B luminescence spectrometer (Norwalk, CT) equipped with thermally controlled cell holder at 22°C. The intensity of the scattered light was measured perpendicular to the incident light. Both the excitation and emission wavelengths were 600 nm with 3-nm slits.

Fluorescence lifetime and emission anisotropy decay measurements

The fluorescence measurements were made with an ISS K2 multifrequency phase fluorometer (ISS Fluorescence Instrumentation, Champaign, IL) using the frequency cross-correlation method. The excitation light was provided by a 300-W Xe arc lamp and was modulated with a double-crystal Pockels cell. Excitation wavelength was set to 350 nm and the emission was monitored through a KV 370 high-pass filter. The modulation frequency was changed in 10 steps (linearly distributed on a logarithmic scale) from 2 to 80 MHz in fluorescence lifetime measurements and from 2 to 150 MHz in anisotropy decay measurements. The phase delay and demodulation of the sinusoidally modulated fluorescence signal were measured with respect to the phase delay and demodulation of a standard reference substance. Freshly prepared glycogen solution was used as a reference (lifetime = 0 ns). The fluorescence lifetimes of the fluorophore were determined by the use of nonlinear least-square analysis. In anisotropy decay measurements the sample was excited with sinusoidally modulated and polarized light. To resolve the anisotropy decay parameters, the difference between the phase angle and modulation ratio of the parallel and perpendicular components of the emission was used. The data were analyzed by the ISS187 decay analysis software assuming a constant, frequency-independent error in both phase angle ($\pm$ 0.200°) and modulation ratio ($\pm$ 0.004). The goodness of fit was determined from the value of the reduced χ^2 defined as in Lakowicz (1983):

$$\chi^2 = \Sigma \frac{[(P_c - P_m)/\sigma^P]^2 + [(M_c - M_m)/\sigma^M]^2}{2n - f - 1} \qquad (1)$$

where the sum is carried over the measured values at n modulation frequencies and f is the number of free parameters. The symbols P and M correspond to phase shift and relative demodulation values, respectively. The indices c and m indicate the calculated and measured values respectively. σ^P and σ^M are the standard deviations of each phase and modulation measurements.

Average fluorescence lifetimes were calculated from the results of the analysis assuming discrete lifetime distribution as described by Lakowicz (1983):

$$\tau_{aver} = (\Sigma\alpha_i\tau_i^2)/(\Sigma\alpha_i\tau_i) \quad (2)$$

where τ_{aver} is the average fluorescence lifetime and α_i and τ_i are the individual amplitudes and lifetimes, respectively. Assuming that the temperature-dependence of the fluorescence of IAEDANS is represented by a single Arrhenius factor, the average fluorescence lifetime was analyzed as a function of temperature according to the equation:

$$(\tau_{aver})^{-1} = k_o + A\ \exp(-E^*/RT) \quad (3)$$

where k_o is the temperature-independent rate constant (both radiative and nonradiative), A is the frequency factor, E^* is the activation energy, T is the absolute temperature, and R is the molar gas constant.

The anisotropy is expected to decay as a sum of exponentials (Belford et al., 1972). The experimentally obtained data were fitted to a double exponential function:

$$r(t) = r_1\exp(-t/\varphi_1) + r_2\exp(-t/\varphi_2) \quad (4)$$

where φ_i are the rotational correlation times with amplitudes r_i. The limiting anisotropy recovered at zero time is given by:

$$r_o = r_1 + r_2 \quad (5)$$

The concentration of actin was 23 μM (1 mg/ml) during the fluorescence measurements. Temperature-dependent experiments were carried out using a thermostated sample holder, which was flushed with dry air to avoid condensation. The temperature was maintained with a HAAKE F3 heating bath and circulator (HAAKE Mess-Technik GmbHu. Co., Karlsruhe, Germany) and the temperature of the solution was continuously monitored in the sample holder.

EPR measurements

Conventional and ST-EPR spectra were taken with an ESP 300E (Bruker, Karlsruhe, Germany) spectrometer. First harmonic, in-phase absorption spectra were obtained using 20 mW microwave power and 100 kHz field modulation with amplitude of 0.1–0.2 mT. Second harmonic, 90° out-of-phase absorption spectra were recorded with 63 mW and 50 kHz field modulation of 0.5 mT amplitude detecting the signals at 100 kHz out of phase. The microwave power of 63 mW corresponds to an average microwave field amplitude of 0.025 mT in the center region of the standard tissue cell of Zeiss (Carl Zeiss, Jena, Germany), and the values were obtained using the standard protocols (Fajer and Marsh, 1982; Squire and Thomas, 1986). The samples ($\sim$ 50 μl) were thoroughly mixed on the surface of the flat cell to avoid the effect of orientation of associated filaments. The spectra were recorded at 22.0°C. The conventional EPR spectra were characterized with the splitting of the outermost extreme ($2A'_{ZZ}$), the accuracy of the estimation of splitting was $<$0.025 mT. In the saturation transfer EPR time domain, the diagnostic peak heights L and L″ were used to calculate the rate of molecular motions. The spectra were scaled to the same peak-to-peak amplitude or normalized to an identical double integral. Evaluation of the ST-EPR spectra was performed by a computer program written in our laboratory that calculates the extremum of the spectrum in a given interval. Varying the endpoints of the selected interval in the neighborhood of the extremum and running the program three to five times, it is possible to get a reliable mean value for L″ and L even in the case of noisy spectra.

RESULTS

The completion of polymerization was tested by light-scattering measurements for both Ca-actin and Mg-actin (Fig. 1). These data indicate that the polymerization process was complete after 4 h and 2 h in the case of Ca-actin and Mg-actin, respectively. Fluorescence lifetimes were measured in Ca^{2+}- or Mg^{2+}-loaded filaments as a function of temperature in five steps ranging from 9 to 33°C. Fluorescence data were analyzed by assuming either discrete or continuous (Gaussian) lifetime distributions. The adequacy of the assumptions was tested by monitoring the value of the reduced χ^2 (Eq. 1). In the case of Gaussian distribution the values of χ^2 were larger than that for the two components discrete analysis in both Mg-F-actin and Ca-F-actin. The analysis assuming discrete components was carried out for one-, two-, or three-exponentials decay model. Better fits were obtained by accepting the two-exponential decay model (with a typical χ^2 of 1.5–2.5) than by assuming a single exponential decay (with χ^2 of 11–19) in both Mg-F-actin and Ca-F-actin. Involving a third lifetime component in the analysis improved χ^2 negligibly. Therefore, in agreement with previous observations (e.g., Ikkai et al., 1979; Miki et al., 1982a,b), the two-exponential fluorescence decay with discrete distribution seems to be the best model for characterizing the fluorescent lifetime of IAEDANS attached to either Ca-F-actin or Mg-F-actin (Table 1).

The average fluorescence lifetime values were calculated for further analysis (Eq. 2, Table 1). This parameter is longer at temperatures below 28.5°C in Ca-F-actin than in Mg-F-actin but the difference disappears at $\sim$ 33°C. As the temperature increased the values of lifetimes decreased in both forms of F-actin; this change was more intense in the

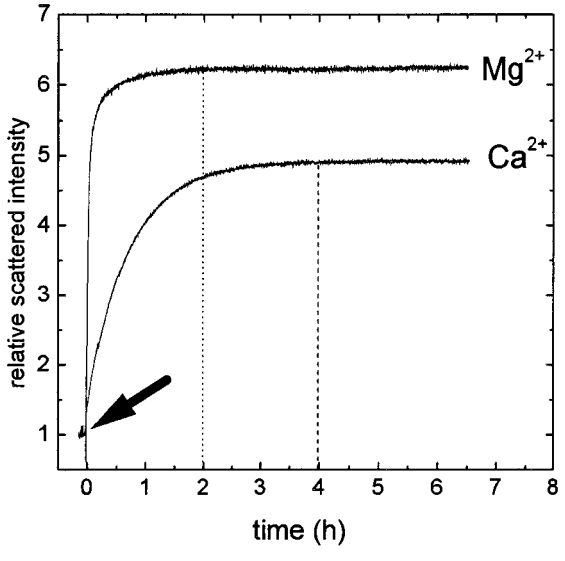

FIGURE 1 The relative intensity of the scattered light as a function of time during the polymerization process in Ca-actin and Mg-actin. Polymerization was initiated by the addition of 100 mM of KCl and 2 mM of the appropriate cation (final concentrations). The arrow indicates the time of addition of salts.

TABLE 1 Lifetime parameters for IAEDANS in Mg-F-actin and Ca-F-actin analyzed with the assumption of two-component discrete distribution of fluorescence decays

Parameter	Mg-F-actin				Ca-F-actin			
t (°C)	τ_1* (ns)	τ_2 (ns)	α_1	$\tau_{average}$ (ns)	τ_1 (ns)	τ_2 (ns)	α_1	$\tau_{average}$ (ns)
9.5	19.63 (± 0.07)	3.11 (± 0.74)	0.984 (± 0.002)	19.58 (± 0.06)	20.64 (± 0.54)	5.49 (± 3.30)	0.972 (± 0.013)	20.51 (± 0.46)
15.0	19.35 (± 0.05)	2.94 (± 0.59)	0.985 (± 0.003)	19.31 (± 0.04)	20.22 (± 0.48)	4.85 (± 2.48)	0.974 (± 0.014)	20.11 (± 0.40)
22.0	19.10 (± 0.04)	3.10 (± 0.41)	0.983 (± 0.002)	19.06 (± 0.03)	19.63 (± 0.23)	4.80 (± 1.57)	0.971 (± 0.010)	19.52 (± 0.18)
28.5	18.86 (± 0.08)	3.37 (± 0.68)	0.980 (± 0.004)	18.80 (± 0.07)	18.97 (± 0.15)	3.33 (± 1.51)	0.980 (± 0.006)	18.91 (± 0.14)
33.0	18.72 (± 0.07)	2.989 (± 0.693)	0.981 (± 0.004)	18.67 (± 0.05)	18.74 (± 0.23)	3.98 (± 1.57)	0.976 (± 0.007)	18.66 (± 0.21)

*τ_1 and α_i are the lifetimes and pre-exponential factors, respectively, where $\alpha_1 + \alpha_2 = 1$. τ_{aver} is the average fluorescence lifetime calculated according to Eq. 1. The standard deviations are presented in parentheses.

Ca^{2+}-loaded than in the Mg^{2+}-loaded form. Arrhenius plots (Eq. 3) were used for further characterization of the temperature-dependence of lifetime values for Mg-F-actin and Ca-F-actin. Plots of $\ln(\tau_{aver}^{-1} - k_o)$ vs. $(RT)^{-1}$ were constructed (e.g., Fig. 2) and the analysis of the fits were made by applying Eq. 3 to calculate the Arrhenius parameters. The k_o was assumed to be cation-independent and was fixed during the fitting procedure. The value of this parameter was changed in 0.01-ns^{-1} steps between 0 and 0.04 ns^{-1} in separate fitting processes (Table 2). It should be noted here that the value of k_o theoretically cannot be larger than ~ 0.05 (see Eq. 3) due to the relatively long fluorescence lifetime of IAEDANS in actin (~ 20 ns). The other components of Eq. 3, A and E*, were taken as variables. The results, relying on the assumption of different k_o values, are shown in Table 2. Accordingly, both the activation energy E* and the frequency factor A are larger in Ca-F-actin than in Mg-F-actin, regardless of the initial assumption of the value of k_o.

To obtain further information about the dynamic properties of actin filaments the fluorescence anisotropy decay was also measured in the temperature range of 9–33°C. The analysis relying on the assumption of two decay components was made to interpret the rotational motion of actin filaments. During the analysis the value of the limiting anisotropy (r_o) was varied as a free parameter and was found to be cation-independent (0.315 ± 0.033 for Mg-F-actin and 0.315 ± 0.026 for Ca-F-actin). The values of the long rotational correlation times are larger in Mg-F-actin than in Ca-F-actin and tend to decrease as the temperature increases (Fig. 3). In contrast to these data for Mg-F-actin the values of this parameter for Ca-F-actin are nearly unchanged. The difference between the longer rotational correlation times measured in Ca-F-actin and Mg-F-actin seems to be negligible above 28°C. The values of shorter rotational correlation times are constant within the limits of experimental errors at all temperatures (ranging between 1 and 3 ns) and are identical for Ca-F-actin and Mg-F-actin (data not shown).

Comparison of conventional EPR spectra obtained on F-actin in Ca- and Mg-state showed no remarkable difference between the hyperfine splitting constants ($2A'_{ZZ}$, Fig. 4). The value of this parameter was ~ 6.67 ± 0.02 mT in both states, which agrees with earlier observations (Thomas et al., 1979, Mossakowska et al., 1988). In contrast, the ST-EPR spectra (Fig. 5) showed a significant difference in the low-field spectral parameter L″/L after the exchange of Ca^{2+} by Mg^{2+} (Table 3). The apparent rotational correlation times corresponding to the spectral parameter L″/L are 65 and 75 μs in Ca-F-actin and Mg-F-actin, respectively (Horváth and Marsh, 1983).

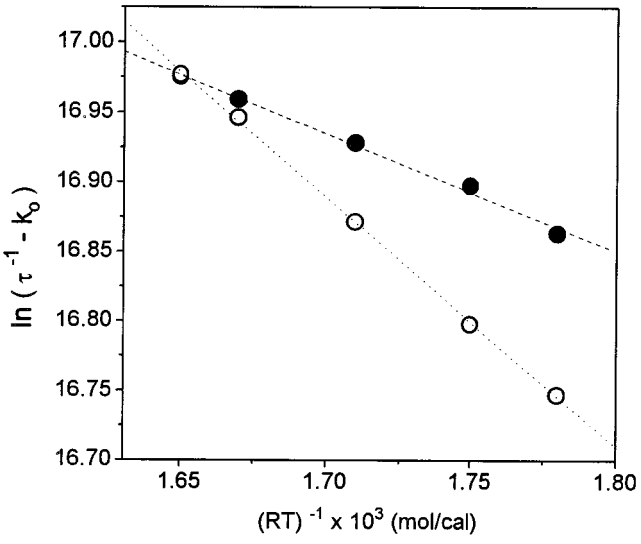

FIGURE 2 Arrhenius plots for the temperature dependence of the measured lifetimes of IAEDANS in Mg-F-actin (*filled symbols*) and Ca-F-actin (*open symbols*). The temperature-independent rate constant (k_o) was taken to be 0.03 ns^{-1} (see also Table 2).

TABLE 2 Arrhenius parameters for the temperature dependence of the measured lifetimes of IAEDANS in Mg- and Ca-F-actin at different k_o values

Parameter	Mg-F-actin		Ca-F-actin	
$k_o \times 10^{-9}$ (s^{-1})	$A \times 10^{-7}$ (s^{-1})	E* (kcal/mol)	$A \times 10^{-7}$ (s^{-1})	E* (kcal/mol)
0.04	14.99 (1.52)	1.46 (0.06)	301.10 (44.76)	3.275 (0.09)
0.03	8.85 (0.05)	0.80 (0.03)	39.56 (3.29)	1.71 (0.05)
0.02	8.62 (0.03)	0.55 (0.02)	22.70 (1.38)	1.16 (0.04)
0.01	8.75 (0.20)	0.42 (0.01)	18.49 (0.89)	0.88 (0.03)
0.00	9.42 (0.12)	0.34 (0.01)	17.13 (0.69)	0.71 (0.02)

Standard deviations are given in parentheses.

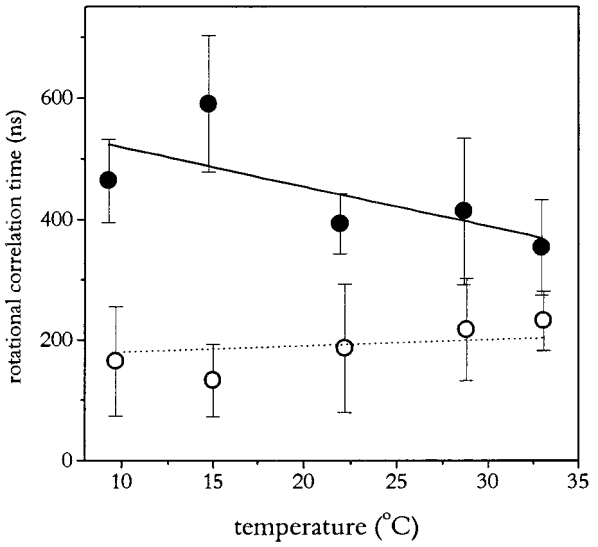

FIGURE 3 Temperature dependence of the longer rotational correlation times of the anisotropy decay of IAEDANS in Mg-F-actin (*filled circles*) and Ca-F-actin (*open circles*).

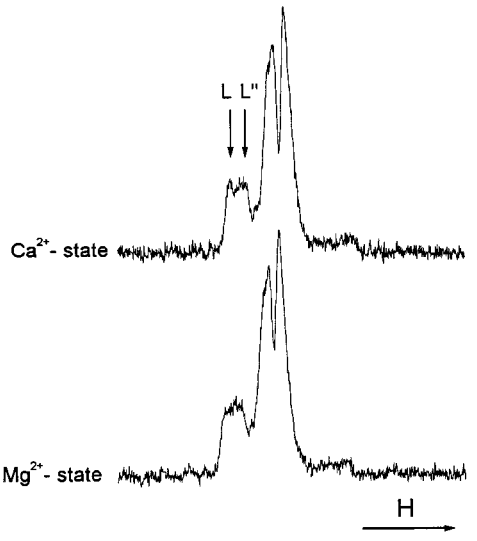

FIGURE 5 ST-EPR spectra of MSL-Ca-F-actin and MSL-Mg-F-actin. The field scan was 20 mT.

DISCUSSION

The fluorescence lifetime of the IAEDANS is longer in the Mg-F-actin than that in Ca-F-actin below 28°C (Table 1). Similar cation dependence of the fluorescence intensity (Frieden et al., 1980) and lifetime (Nyitrai et al., 1997) of IAEDANS was observed in the monomeric forms of actin as well. Frieden and colleagues concluded from the cation-induced intensity change that there is a conformational difference between the C-terminal segment of the Ca^{2+}- and Mg^{2+}-saturated forms of the monomer (Frieden et al., 1980). In the light of the data presented here, one can conclude that this conformational difference is conserved to a certain extent during polymerization.

The Arrhenius plots were applied to interpret the temperature dependence of the average fluorescent lifetimes in the Ca-F-actin and Mg-F-actin (Eq. 3). Such an analysis can provide information about the microenvironment of the reporter molecule. According to our data both the activation energy (E^*) and the frequency factor (A) are larger in the case of Ca-F-actin than in the case of Mg-F-actin (Table 3), indicating that the protein matrix around the Cys^{374} residue is more rigid in the Mg^{2+}-saturated form of the actin filament. Similar cation induced change in the flexibility was reported recently for actin monomers as well (Strzelecka-Golaszewska et al., 1993; Nyitrai et al., 1997). These data imply, in agreement with the conclusion derived from the results of fluorescence lifetime experiments, the conservation of the cation-dependent flexibility difference of the protein matrix around the Cys^{374} residue after polymerization. Three-dimensional reconstructions from electron micrographs have showed that a bridge of density exists between the two strands of the filament in Ca-actin that is absent in Mg-actin (Orlova and Egelman, 1995). According to the interpretation of these authors, this bridge of density arises from a major shift of the C terminus. Accordingly, the cation-induced difference in the flexibility of the microen-

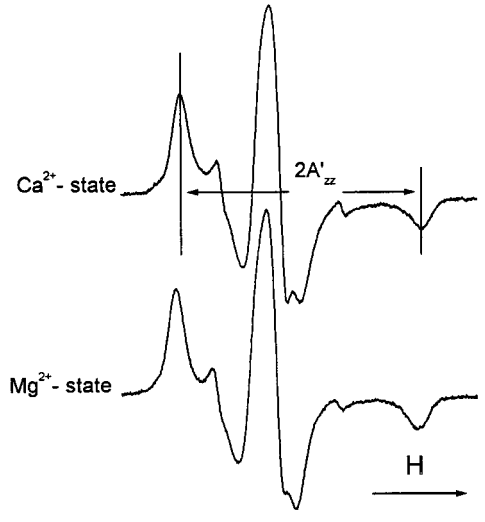

FIGURE 4 Conventional EPR spectra of Ca-F-actin and Mg-F-actin. The concentration of actin was 167 μM and field scan was 10 mT. Actin was labeled with MSL at the Cys^{374} site.

TABLE 3 Conventional and saturation transfer EPR spectral parameters of spin-labeled actin (MSL-actin) upon the replacement of Mg^{2+} by Ca^{2+}

Parameter	Ca-F-actin	Mg-F-actin
Conventional EPR	6.760	6.763
$2A'_{zz}$ (mT)	(± 0.025) (n = 10)	(± 0.022) (n = 9)
ST-EPR	0.966	1.067
L″/L	(± 0.067) (n = 8)	(± 0.055) (n = 8)

Standard deviations are presented in parentheses.

vironment of Cys^{374} in actin filaments might reflect the presence of the proposed high-density bridge between the two strands of the Ca-F-actin.

The difference in the local dynamic properties of the protein matrix around Cys^{374} may reflect a modification of a larger segment or the entire filament as a result of the cation exchange. In order to characterize global changes induced by cations, the anisotropy decay of the IAEDANS was also investigated. The longer rotational correlation times are in agreement with the values obtained by Miki and co-workers who found $\varphi_2 = 260$ ns for Ca-F-actin and $\varphi_2 = 682$ ns for Mg-F-actin at 20°C labeled with IAEDANS at Cys^{374} (1982b).

The components of the anisotropy decay can potentially characterize different regions of the actin filament. The interpretation of the long component (φ_2) resolved in these experiments is critical. This parameter obviously cannot be specific for the rotation of the whole filament because this rotation has to be much slower than the one indicated by the longer correlation time. Furthermore, the bending motion of the filament was found to occur with about 10-ms correlation times (Fujime and Ishiwata, 1971); thus, the contribution of this kind of motion should also be unnoticed in our experiments. The longer correlation times may be attributed to some restricted segmental motion in the filament (Ikkai et al., 1979; Miki et al., 1982a,b). The segment may be the protomer, but smaller components of actin cannot be ruled out as contributors to this correlation time. The value of the longer correlation time is assumed to be inversely proportional to the flexibility of the actin filaments (Tawada et al., 1978; Ikkai et al., 1979; Miki et al., 1982a,b; Hegyi et al., 1988). The decrease in this correlation time may be the result of loosening of the physicochemical links between adjacent protomers in the actin filament. Accordingly, the results of the fluorescence anisotropy decay experiments support the view that cation exchange induces conformational transition within the actin filament, resulting in a more rigid form of Mg-F-actin compared to Ca-F-actin.

Inspection of the conventional EPR spectra obtained on Ca-F-actin and Mg-F-actin revealed essentially no difference between the hyperfine splitting constants ($2A'_{ZZ}$, Fig. 4). This observation suggests the absence of a detectable change in rotational mobility on the nanosecond time scale as a result of the exchange of Ca^{2+} by Mg^{2+} (Table 3). The spin labels are sensitive reporters of the polarity of the microenvironment around the binding site as well. The slight change of the splitting constant upon replacement of Ca^{2+} with Mg^{2+} shows that the exchange of cations does not remarkably affect the polarity of the medium. This conclusion is apparently not in agreement with the results of fluorescence experiments. According to earlier publications (e.g., Stryer, 1968), the origin of this conflict might be the difference between the fluorescence and EPR methods. Furthermore, different reporter molecules were used to study the protein matrix in the two methods, and the difference between the mobility of these labels might also contribute to the difference in the observations. According to earlier data (Thomas et al., 1979), in contrast to the fluorescent probes, the maleimide spin labels are rigidly attached to the Cys^{374} residue of the actin protomer; the probe mobility relative to the protein backbone can be neglected, thus the probe molecules in F-actin report slow domain motions.

However, comparison of the spectral parameter L″/L resolved in the ST-EPR experiments showed that the local protein environment of the probe becomes more rigid after Mg^{2+} is replaced by Ca^{2+} at the high-affinity cation binding site. The inspection of the rotational dynamics of F-actin by ST-EPR experiments suggests that a complex motion is observed, which may be a superposition of twisting and torsional motions of the actin filament or a larger part of the filament (Thomas et al., 1979). Therefore, the motion of the labels in actin filaments reflects more than one mode of motion, and their motion is not isotropic. Accordingly, the apparent rotational correlation times demonstrate only the magnitude of the rotational motion of the labels in filament forms of actin in the ST time range. The apparent rotational correlation times are on the order of 10^{-4} s, much smaller than the bending motion of the entire filament and much larger than that of the overall monomer rotation; they should represent a complex intrafilament motion involving different modes. However, based on these data one cannot distinguish between the possibilities that the structure is more flexible along its entire length and that it possesses restricted regions. The change of internal flexibility induced by the exchange of Ca^{2+} for Mg^{2+} in monomer actin has been interpreted as a change in the angularly restricted motion of the label (Nyitrai et al., 1997). The increase of rotational correlation time may imply that the effect of exchange of cations in F-actin can propagate to distant parts of the protomers inducing a change of rigidity in the internal region of the protomers and/or between neighboring protomers. The interaction between the protomers might be modulated by the conformational state of the actin subunits, and the exchange of cations can stabilize the interactions between the two helical strands. This can lead to an increase of the rotational correlation time. Comparing the EPR and the fluorescence data, the more likely interpretation is that intermonomer interaction is stronger in the Mg^{2+}-saturated filament than in the Ca^{2+}-saturated form due to the increasing restriction of the twisting and torsional motions of the individual protomers.

These conclusions do not seem to agree with results obtained by other experimental methods (Orlova and Egelman, 1993; Isambert et al., 1995; Scharf and Newman, 1995; Yasuda et al., 1996; Steinmetz et al., 1997). These studies found the flexibility of Mg^{2+}-saturated actin filaments identical to (Isambert et al., 1995; Scharf and Newman, 1995; Yasuda et al., 1996; Steinmetz et al., 1997) or larger than (Orlova and Egelman, 1993) that of filaments polymerized from Ca-actin. Steinmetz and co-workers (1997) have suggested that different methods of polymerization applied by different laboratories might be responsible for the conflicting conclusions. Our present data indicate that the Mg^{2+}-loaded filaments are more rigid than the

filaments of Ca-actin. To explain the difference between this conclusion and the results cited above, one needs to consider that the earlier conclusions were based on investigations of slower motions (e.g., the bending of actin filaments) appearing on a 1-ms or longer time scale. The motion characterized in our fluorescence anisotropy and saturation transfer EPR experiments is much faster than the bending motions of filaments. Accordingly, it is not surprising that the cation-induced changes resolved by the different methods do not correlate.

CONCLUSIONS

Combining fluorescence lifetime experiments and the Arrhenius analysis enabled us to distinguish between Ca-F-actin and Mg-F-actin, indicating that the conformation and/or flexibility of the protein region around the Cys^{374} residue is sensitive to the nature of the bound cation. Based upon our data, obtained from both fluorescence anisotropy decay and ST-EPR experiments, the actin filaments appear to be more rigid when Mg^{2+} binds to the high-affinity cation-binding sites than in the case of Ca^{2+}-loaded actin. Changes in the molecular properties of the actin molecule due to the effect of Ca^{2+} ion binding can be important in different ways in the function of the muscle cells. In resting muscle cells, the Mg^{2+} ions are thought to occupy the high-affinity cation-binding sites in F-actin. We can speculate that the exchange of Mg^{2+} for Ca^{2+} during muscle contraction could enhance the activity, allowing larger structural fluctuations in the thin filaments.

Knowledge of the structure of actin in its various conformational states is important for understanding the diverse motile activities in biological systems. This statement is supported by recent suggestions about the role of actin in the force development of muscle. The actin powerstroke model is based on the length changes in actin filaments that require conformational transitions in each monomer (Schutt et al., 1995). The large free-energy change upon binding of the myosin head to actin is also able to generate conformational change in actin (Geeves, 1991). During the ATP hydrolysis cycle the myosin heads can adopt more than one conformation in interaction with actin, the multiple modes of binding can relate to different actin conformations. The exchange of Ca^{2+} by Mg^{2+} is accompanied by a change in the intramolecular motion of the actin filament, which can increase the elastic resistance to deformation. It is known that the *N*-terminal region of the LC1 light chain of myosin interacts directly with the C-terminal region of actin (Trayer et al., 1987). The altered conformation of actin might modulate the segmental mobility of the light chain that effects the force generation process.

It is important to note that the cation-induced change in filament flexibility can be the result of change in either intermonomer bonding or intramonomer flexibility. From the experimental results presented here it was not possible to identify which of these changes contribute to the flexibility difference found between the Ca-F-actin and Mg-F-actin. The separation of the cation-induced modification of intramonomer and intermonomer flexibility seems to be possible using the method of fluorescence resonance energy transfer (Somogyi et al., 1984). Such experiments are currently in progress in our laboratory.

This work was supported by the National Research Foundation (OTKA Grants T017727, T023209, F020174, and T017099), by the Ministry of Public Health and Welfare (Grant ETT T-06017/96), and by the Hungarian Academy of Sciences.

REFERENCES

Belford, G. G., R. L. Belford, and G. Weber. 1972. Dynamics of fluorescence polarization in macromolecules. *Proc. Natl. Acad. Sci. USA.* 69(6):1392–1393.

Elzinga, M., J. H. Collins, W. M. Kuehl, and R. S. Adelstein. 1973. Complete amino-acid sequence of actin of rabbit skeletal muscle. *Proc. Natl. Acad. Sci. USA.* 70:2687–2691.

Fajer, P., and D. Marsh. 1982. Microwave and modulation field inhomogenities and effect of cavity Q in saturation transfer EPR spectra: dependence of sample size. *J. Magn. Reson.* 49:212–224.

Feuer, G., F. Molnár, E. Pettkó, and F. B. Straub. 1948. Studies on the composition and polymerisation of actin. *Hung. Acta Physiol.* I:150–163.

Frieden, C., D. Lieberman, and H. R. Gilbert. 1980. Fluorescence probe for conformational changes in skeletal muscle G-actin. *J. Biol. Chem.* 255: 8991–8993.

Fujime, S., and S. Ishiwata. 1971. Dynamic study of F-actin by quasielastic scattering of laser light. *J. Mol. Biol.* 62:251–265.

Geeves, M. A. 1991. The dynamics of actin and myosin association and the crossbridge model of muscle contraction. *Biochem. J.* 274:1–14

Hegyi, Gy., L. Szilágyi, and J. Belágyi. 1988. Influence of the bound nucleotide on the molecular dynamics of actin. *Eur. J. Biochem.* 175: 271–274.

Heintz, D., H. Kany, and H. R. Kalbitzer. 1996. Mobility of the N-terminal segment of rabbit skeletal muscle F-actin detected by 1H and 19F nuclear magnetic resonance spectroscopy. *Biochemistry.* 35: 12686–12693.

Horváth, L. I., and D. Marsh. 1983. Analysis of multicomponent saturation transfer ESR spectra using integral method: application to membrane systems. *J. Magn. Reson.* 54:363–373.

Houk, W. T., and K. Ue. 1974. The measurement of actin concentration in solution: a comparison of methods. *Anal. Biochem.* 62:66–74.

Hudson, E. N., and G. Weber. 1973. Synthesis and characterization of two fluorescent sulfhydryl reagents. *Biochemistry.* 12:4154–61.

Ikkai, T., P. Wahl, and J. C. Auchet. 1979. Anisotropy decay of labeled actin. Evidence of the flexibility of the peptide chain in F-actin molecules. *Eur. J. Biochem.* 93:397–408.

Isambert, H., P. Venier, A. C. Maggs, A. Fattoum, R. Kassab, D. Pantaloni, and M.-F. Carlier. 1995. Flexibility of actin filaments derived from thermal fluctuations. *J. Biol. Chem.* 270(19):11437–11444.

Kawamura, M., and K. Maruyama. 1970. Electron microscopic particle length of F-actin polymerized in vitro. *J. Biochem. (Tokyo).* 67: 437–457.

Kawasaki, Y., K. Mihashi, H. Tanaka, and H. Ohnuma. 1976. Fluorescence study of N-(3-pyrene)maleimide conjugated to rabbit skeletal F-actin and plasmodium actin polymers. *Biochim. Biophys. Acta.* 446:166–178.

Lakowicz, J. R. 1983. Measurements of fluorescence lifetimes. *In* Principles of Fluorescence Spectroscopy. Plenum Press, New York and London. 52–95.

Mihashi, K., H. Yoshimura, T. Nishio, A. Ikegami, and K. Kinosita, Jr. 1983. Internal motion of F-actin in 10^{-6}-10^{-3} s time range studied by transient absorption anisotropy: detection of torsional motion. *J. Biochem. (Tokyo)* 93:1705–1707.

Mihashi, K., and P. Wahl. 1975. Nanosecond pulsefluorometry in polarized light of G-actin-epsilon-ATP and F-actin-epsilon-ADP. *FEBS Lett.* 52: 8–12.

Miki M., C. G. dos Remedios, and J. A. Barden. 1987. Spatial relationship between the nucleotide-binding site, Lys-61 and Cys-374 in actin and a conformational change induced by myosin subfragment-1 binding. *Eur. J. Biochem.* 168:339–345.

Miki, M., P. Wahl, and J.-C. Auchet. 1982a. Fluorescence anisotropy of labeled F-actin: Influence of Ca^{2+} on the flexibility of F-actin. *Biophys. Chem.* 16:165–172.

Miki, M., P. Wahl, and J.-C. Auchet. 1982b. Fluorescence anisotropy of labeled F-actin: Influence of divalent cations on the interaction between F-actin and myosin heads. *Biochemistry.* 21:3661–3665.

Mossakowska, M., J. Belágyi, and H. Strzelecka-Golaszewska. 1988. An EPR study of the rotational dynamics of actins from striated and smooth muscle and their complexes with heavy meromyosin. *Eur. J. Biochem.* 175:557–564.

Nyitrai, M., G. Hild, J. Belágyi, and B. Somogyi. 1997. Spectroscopic study of conformational changes in subdomain 1 of G-actin: influence of divalent cations. *Biophys. J.* 73:2023–2032.

Orlova A., and E. H. Egelman. 1993. A conformational change in the actin subunit can change the flexibility of the actin filament. *J. Mol. Biol.* 232:334–341.

Orlova A., and E. H. Egelman. 1995. Structural dynamics of F-actin: I. Changes in the C terminus. *J. Mol. Biol.* 245(5):582–97.

Prochniewicz, E., and T. Yanagida. 1990. Inhibition of sliding movement of F-actin by cross-linking emphasizes the role of F-actin structure in the mechanism of motility. *J. Mol. Biol.* 216:761–772.

Rayment, I., H. Holden, M. Whittaker, C. B. Yohn, M. Lorenz, K. C. Holmes, and R. A. Milligan. 1993. Structure of the actin-myosin complex and its implications for muscle contraction. *Science.* 261:58–65.

Scharf, R. E., and J. Newman. 1995. Mg- and Ca-actin filaments appear virtually identical in steady-state as determined by dynamic light scattering. *Biochim. Biophys. Acta.* 1253:129–132.

Schutt, C. E., M. D., Rozycki, J. K., Chick, and U. Lindberg. 1995. Structural studies on the ribbon-to-helix transition in profilin: actin crystals. *Biophys. J.* 68:12s–18s.

Somogyi, B., J., Matkó, S., Papp, J., Hevessy, G. R., Welch, and S., Damjanovich. 1984. Förster-type energy transfer as a probe for changes in local fluctuations of protein matrix. *Biochemistry.* 23:3403–3411.

Spudich, J. A., and S. Watt. 1971. The regulation of rabbit skeletal muscle contraction. I. Biochemical studies of the interaction of the tropomyosin-troponin complex with actin and the proteolytic fragments of myosin. *J. Biol. Chem.* 246:4866–4871.

Squire, T. C., and D. D. Thomas. 1986. Methodology for increased precision in saturation transfer electron paramagnetic resonance studies of rotational dynamics. *Biophys. J.* 49:921–935.

Steinmetz, M. O., K. N. Goldie, and U. Aebi. 1997. A correlative analysis of actin filament assembly, structure and dynamics. *J. Cell Biol* 138: 559–574.

Stryer, L. 1968. Fluorescence spectroscopy of proteins. *Science.* 162: 526–533.

Strzelecka-Golaszewska, H., J. Moraczewska, S. Y. Khaitlina, and M. Mossakowska. 1993. Localization of the tightly bound divalent-cation-dependent and nucleotide-dependent conformation changes in G-actin using limited proteolytic digestion. *Eur. J. Biochem.* 211:731–742.

Tawada, K., P. Wahl, and J.-C. Auchet. 1978. Study of actin and its interaction with heavy meromyosin and regulatory proteins by the pulse fluorimetry in polarized light of a fluorescent probe attached to an actin cysteine. *Eur. J. Biochem.* 88:411–419.

Thomas, D. D., J. C. Seidel, and J. Gergely. 1979. Rotational dynamics of spin-labeled F-actin in the sub-millisecond time range. *J. Mol. Biol.* 132:257–273.

Trayer, I. P., H. R., Trayer, and B. A Levine. 1987. Evidence that the N-terminal region of A1-light chain of myosin interacts directly with the C-terminal region of actin. *Eur. J. Biochem.* 164:259–266.

Wahl, P., K. Mihashi, and J. C. Auchet. 1975. Nanosecond pulse fluorometry in polarized light of dansyl-L-cysteine linked to a unique SH group of F-actin; the influence of regulatory proteins and myosin moiety. *FEBS Lett.* 60:164–167.

Yasuda, R., H. Miyata, and K. Kinosita Jr. 1996. Direct measurement of torsional rigidity of single actin filaments. *J. Mol. Biol.* 263:227–236.